

Modeling defects in Nb<sub>3</sub>Sn Superconductor Resonance Cavities with Ginzburg-Landau Theory

Braedon Jones

A senior thesis submitted to the faculty of  
Brigham Young University  
In partial fulfillment of the requirements for the degree of

Bachelor of Science

Mark K. Transtrum

Department of Physics and Astronomy

Brigham Young University

April 2021

Copyright © 2021 Braedon Jones

All Rights Reserved



## ABSTRACT

### Modeling Nb<sub>3</sub>Sn Superconductor Using Ginzburg-Landau Equations

Braedon Jones

Department of Physics and Astronomy

Bachelor of Science

Superconducting resonance cavities are used in particle accelerators to accelerate beams of charged particles to near light speed. The fundamental limit to performance in these cavities is the maximum induced magnetic field that the superconductors can expel due to the Meissner effect. Traditionally, cavities have been made from Niobium; however, current technology has nearly reached the theoretical limit of performance for Niobium-based cavities. To overcome these limitations, Nb<sub>3</sub>Sn is being explored as a potential next-generation material. In actual development of Nb<sub>3</sub>Sn cavities, material defects arise that may limit performance. Time-dependent Ginzburg-Landau simulate deficiencies to explore if they cause detrimental effects to cavity performance. This research focuses on small ‘island’ regions containing deficits of Sn. These islands have been observed below the surface in real Nb<sub>3</sub>Sn cavities after fabrication. This research shows that these islands may affect performance if they are near the surface but become irrelevant when they are located more than a penetration depth below the interface.

Keywords: Nb<sub>3</sub>Sn, Ginzburg-Landau, Superconductors, Magnetic Fields

# Acknowledgments

---

My parents have played a large role throughout my life and have always desire the best for me.

My sister and brothers are inspirations because of their hard-working examples. I am grateful for

Dr. Mark K. Transtrum for his time, patience, and teachings. I also am thankful towards the rest

of the BYU faculty who have dedicated so much for my classes and studies throughout my time

in college, without whom, I would not be where I am today.

# Table of Contents

---

Table of Contents.....	v
List of Figures.....	vii
List of Tables.....	viii
<b>1 Introduction .....</b>	<b>9</b>
1.1 Motivation.....	9
1.2 Background .....	9
1.2.1 Meissner Effect .....	9
1.2.2 Type I/Type II Superconductors:.....	10
1.2.3 Alternate Materials:.....	12
1.3 Previous Research at BYU.....	13
1.4 Overview.....	13
<b>2 Methods .....</b>	<b>14</b>
2.1 Ginzburg-Landau Equations: .....	14
2.2 Finite Element Mesh:.....	16
2.3 Alpha Islands: .....	16
2.4 Saddle Node Bifurcation to Locate Hsh: .....	17
2.5 Overview.....	19
<b>3 Results and Conclusions.....</b>	<b>19</b>

3.1	<i>Results</i> .....	20
3.1.1	Island Size Variations: .....	20
3.1.2	Alpha Size Variations: .....	22
3.1.3	Boundary Condition Variations:.....	23
3.2	<i>Conclusion</i> .....	25
3.3	<i>Future Work</i> .....	26
4	<b>Index</b> .....	<b>28</b>
5	<b>Bibliography</b> .....	<b>29</b>

# List of Figures

---

<b>Figure 1</b> Graph representing the change in state of a superconducting material .....	12
<b>Figure 2</b> The varying levels of $\alpha$ .....	17
<b>Figure 3</b> Generic case of different simulations ran at different applied magnetic fields. ....	18
<b>Figure 4</b> A plot of the distance the island defect is from the material boundary with the Superheating field (Hsh) for different island sizes. ....	21
<b>Figure 5</b> Plots of Distances versus Super Heating Field with $\alpha$ differing from 0 to .75.....	23
<b>Figure 6</b> Boundary Slope Plot.....	24
<b>Figure 7</b> Distance vs Hsh with changing Boundary Slope values. ....	25

# List of Tables

---

**Table 1** List of superconductor parameters for selected materials.....10



# 1 Introduction

---

## 1.1 Motivation

Frequently, particle accelerators work through the application of high electromagnetic fields. To conserve energy and promote resonance, these fields are maintained in superconducting resonance cavities (SRF cavities). This is because superconductors completely repel magnetic fields. However, superconducting materials require extremely low temperatures to remain in their superconducting state. At temperatures above their critical temperature, superconductors act as regular metals, and their utility is lost. Commonly, physicists use expensive cryogenic refrigerators to maintain cavities at low temperatures of around two kelvins. These factors serve as barriers to the proliferation of particle accelerators around the world and the increased study of particles in industry or university environments. Physicists have identified Nb<sub>3</sub>Sn as a potential alternate material of which to construct SRF cavities because of its higher critical temperature and other properties. This would reduce costs of particle accelerators; however, Nb<sub>3</sub>Sn is inhomogeneous when made and requires further probing to determine if it is a viable replacement candidate.

## 1.2 Background

### 1.2.1 Meissner Effect

Superconductors are unique because of the Meissner effect. This is a phenomenon where all the magnetic fields are expelled from the superconductor. Sometimes when a material cools, not all of the magnetic fields are expelled, and some fields (vortices) become trapped within the

material. When a magnetic field is imposed on a material, surface currents form that act to prevent the magnetic field from entering the material. Another incredibly useful characteristic of superconductors is that they have zero resistance. Because of this, the surface currents can perpetually exist to expulse all magnetic fields. When a magnetic field is imposed, it exponentially decays because of the surface currents. The point where the magnetic field has decayed to  $1/e$  of its original value characterizes the London penetration depth ( $\lambda$ ). This parameter varies depending on the superconducting material [1]. Some values for  $\lambda$  can be found in Table 1.

<i>Material</i>	$H_c$ (tesla)	$\lambda$ (nm)	$\zeta$ (nm)	$\kappa$	$T_c$ (K)
Nb	.82	50	22	2.27	9.76
Nb <sub>3</sub> Sn	30	111	4.2	26.4	18.3
Sn	.003	5.0	240	.021	3.72
MgB <sub>2</sub>	74	185	4.9	37.76	37

**Table 2** List of superconductor parameters for selected materials.

### 1.2.2 Type I/Type II Superconductors:

When exposed to a high enough magnetic field, the surface currents are not strong enough to fully repulse the field, and the exterior magnetic field enters. This leads to the material losing its superconducting qualities. Depending on the material, different phenomenon can occur. In general, once the material experiences a magnetic field that surpasses the critical field the material behaves as a normal metal. For materials characterized as Type I superconductors, any penetration of the magnetic field leads to the whole material to immediately behave as a normal metal, and this occurs at the superheating field  $H_{sh}$ . For Type II superconductors, a different phenomenon occurs. When the applied field is equivalent or above  $H_{sh}$ , the material enters a

mixed state where pockets, or vortices, of magnetic field enter. Only in these pockets of magnetic field does the material not behave as a superconductor. The material is said to have quenched when a vortex of magnetic field enters the material. When a Type II superconductor experiences a field greater than  $H_{c2}$ , the material leaves the mixed state for the normal state, and all the material behaves as a normal metal. Figure 1 displays the various states a material can be in depending on the applied magnetic field and the value  $\kappa$ .

What distinguishes Type I superconductors from Type II is the parameter  $\kappa$ , see Table 1, which is the ratio of  $\lambda$  and  $\zeta$ , with  $\zeta$  representing the Coherence length. The Coherence length shows how quickly the order parameter in the Ginzburg-Landau equations vary. A material with a  $\kappa$  value below  $1/\sqrt{2}$  is a Type I superconductor while a material with a value greater than  $1/\sqrt{2}$  is a Type II superconductor.

In both Type I and Type II there exists a meta-stable state, and this occurs when the applied field level surpasses  $H_c$  for Type I superconductors and  $H_{c1}$  for Type II superconductors. This is where the material should begin to leave the superconducting state for a normal state but does not because of other factors. A metastable state is comparable to when water is heated to temperature above the boiling point yet does not boil because of the surface tension of the water. [4]. A disturbance is necessary to break the tension and cause the water to boil. For superconductors it is favorable for magnetic field to penetrate the material, but the material still maintains the magnetic field outside. Some type of disturbance or a higher applied field is necessary for the material to enter the normal state.

Our area of interest is the boundary between the meta-stable state and the mixed state. Nb<sub>3</sub>Sn is a Type II superconductor and experiences the mixed state. Particle accelerators, to

maximize performance, operate with fields just below  $H_{sh}$  so that the superconductor remains in the meta-stable state. Nb3Sn because of its inhomogeneities could have lower values of  $H_{sh}$  than initially thought and this could alter if it is chosen over Nb as the material for SRF cavities.

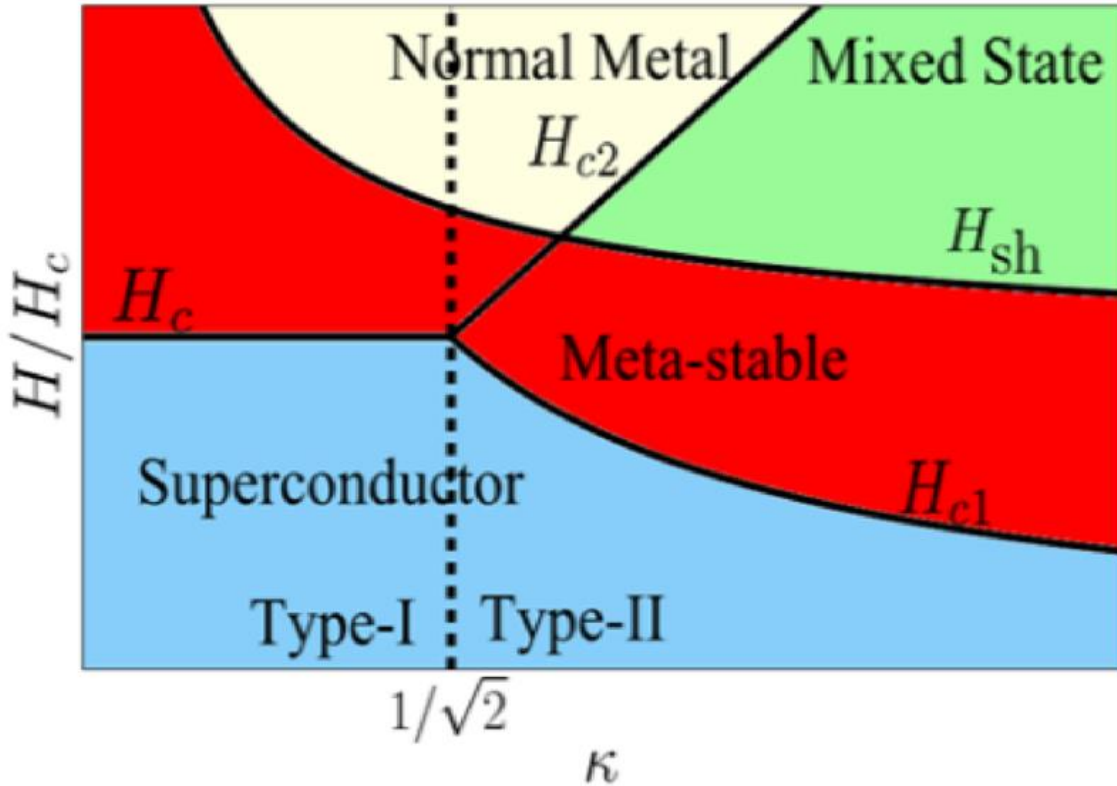


**Figure 1** Graph representation of the change in state of a superconducting material depending on  $\kappa$  and magnetic field. To specify,  $\kappa$  is the ratio of penetration depth and coherence length. Type-I superconductors occur below a  $\kappa$  of  $1/\sqrt{2}$ , and Type-2 occur above  $1/\sqrt{2}$  [2].

### 1.2.3 Alternate Materials:

Niobium has been a common material used to produce SRF cavities; however, it has reached its theoretical limits in application. Niobium itself is a Type II superconductor. Nb3Sn is a Type II super conductor yet has a larger  $\kappa$  value than Niobium. This combined with the fact that Nb3Sn has twice as high of a critical temperature as does Niobium, as can be seen in Table 1, has caused it to be the subject of further study as a potential replacement for Niobium.

Complications occur because fabricating layers of Nb<sub>3</sub>Sn on a SRF cavity does not produce purely homogenous Nb<sub>3</sub>Sn. In the process, defects such as grain boundaries and tin deficiencies are found within the material. A paper by Posen and Hall [3] contains an image of a physical example of such inhomogeneities. In determining if Nb<sub>3</sub>Sn is a viable candidate as a replacement, it must be concluded whether these inhomogeneities have a detrimental effect on superconducting performance of the whole material. This research particularly investigates how Tin island deficiencies effect results.

### **1.3 Previous Research at BYU**

Research consisted of the formulation of the Ginzburg-Landau equations into code through a FEM method by FEniCS. After coding, tests were run to ensure the validity of the simulations [5]. Parameters and complex geometries were added to help replicate computationally superconductors as they occur naturally in SRF cavities [6]. Some research investigated grain boundaries [4]. This project studies Sn island deficiencies.

### **1.4 Overview**

Particle accelerators utilize electromagnetic fields to accelerate particles. They require SRF cavities to contain these fields, and these cavities are made with superconducting materials. Niobium is commonly used to construct the cavity, but it has reached its theoretical limit as a material of the particle accelerator. This, in addition to the super low temperature requirement, has caused scientist to look for potential alternatives. Nb<sub>3</sub>Sn can serve as a great replacement, but this needs to be verified, especially since during fabrication islands and grain boundaries form. These defects could potentially diminish the performance of the superconductor. To test

this, the Ginzburg-Landau equations are written into code to simulation performance. These simulations will help find the maximum magnetic field level, known as the critical field, where Nb3Sn will continue to behave as a superconductor.

## 2 Methods

---

Nb3Sn is a potential alternative for Nb in SRF cavities, but during the development of the cavity, material inhomogeneities occur, including Sn deficient islands. Previously performed quantum calculations determined the superconducting properties of a material, such as the London penetration depth and Coherence length. We then combine the material parameters with the Ginzburg-Landau model of superconductivity to infer cavity performance. The model is implemented computationally on a supercomputer to find the superheating field of a system with a given distribution of material parameters.

### 2.1 Ginzburg-Landau Equations:

The Ginzburg-Lambda equations are a phenomenological model of superconductivity. They accurately describe a superconductor near its critical temperature  $T_c$ . These equations originate from a Taylor approximation of the free energy. The equations minimize the free energy of the material by taking its variational derivative and equating it to zero. The derivation of the equations is better explained in “Introduction to Superconductivity” by Michael Tinkham [6]. The primary equation is the following expression for the free energy:

$$f = f_{n0} + \alpha|\psi|^2 + \frac{\beta}{2}|\psi|^4 + \frac{1}{2m} \left| \left( \frac{\hbar}{i} \nabla - \frac{e}{c} \mathbf{A} \right) \psi \right|^2 + \frac{|\mathbf{h}|^2}{8\pi} \quad (1)$$

The symbol  $\psi$  represents the Order Parameter. When  $\psi$  goes to one, it represents when a material behaves as a superconductor, but when  $\psi$  decreases to zero, this characterizes when the material behaves as a normal metal. The mass of the particle is represented by  $m$ , the charge by  $e$ , and the speed of light by  $c$ . The value  $f_n$  is the free energy when the material acts as a normal metal. The equations also incorporate the total magnetic field  $\mathbf{h}$  and the magnetic potential  $\mathbf{A}$ .

A new form of the equation is found by performing a functional derivative and assuming spatial inhomogeneities in material parameters.

$$0 = \alpha\psi + \beta|\psi|^2\psi + \frac{1}{2m} \left( \frac{\hbar}{i} \nabla - \frac{e}{c} \mathbf{A} \right)^2 \quad (2)$$

Of note here are the material parameters of  $\alpha$  and  $\beta$ . For purposes here  $\beta$  is constant since it does not vary significantly spatially. The variables  $\alpha$  and  $\beta$  play roles in showcasing the superconducting material properties of the material. Tinkham has equations to formulate  $\alpha$  and  $\beta$ :

$$\alpha \propto \frac{1 - t^2}{1 + t^2} \approx \left( 1 - \frac{T}{T_c} \right) \quad (3)$$

$$\beta \propto \frac{1}{(1 + t^2)^2} \approx \text{constant} \quad (4)$$

The value  $T$  is the temperature of the environment and  $T_c$  is the critical temperature where the material loses its superconducting properties. When  $T = T_c$ ,  $\alpha$  is 0. Inhomogeneities cause a lower  $T_c$  and  $\alpha$  converges to zero at a lower temperature than does pure substances. Therefore, the Sn-deficiency islands have lower values for  $\alpha$ .

For simplicity,  $\alpha$  was chosen based off of pure Nb<sub>3</sub>Sn having higher superconducting properties than Sn-deficient Nb<sub>3</sub>Sn. This decision will give inexact results but will still produce expected patterns for the inhomogeneities. To further the discussion, a set of simulations varied the levels of  $\alpha$  as will be explained further in chapter 3.

## **2.2 Finite Element Mesh:**

The Ginzburg-Landau Equation equations have no closed-form solutions. We use Python to solve these equations computationally on the supercomputer. The code incorporates a Finite Element Method (FEM), that discretizes the domain and solves the equations for each point. We implement this method in an open-source solver called FEniCs. It has a Python interface to a C++ library. This simplifies manual coding while still maintaining faster computations.

## **2.3 Alpha Islands:**

As discussed, the scope of this project investigates how defects of the material effect performance of superconducting cavities. In these simulations, we consider a region of higher material superconductivity surrounded by an area of lower superconductivity. The parameter  $\alpha$  distinguishes the materials from one another. An  $\alpha$  value of one characterizes the bulk material Nb<sub>3</sub>Sn. For Sn deficient regions,  $\alpha$  is set to a value less than one. Thus, the islands lacking in Sn are forced to have an  $\alpha$  value less than one, since they have lesser superconducting properties. By varying  $\alpha$  spatially, we created the island geometry as seen in in figure 1. An ellipse of lower



$\alpha$  levels is surrounded by a material with pure superconducting properties.

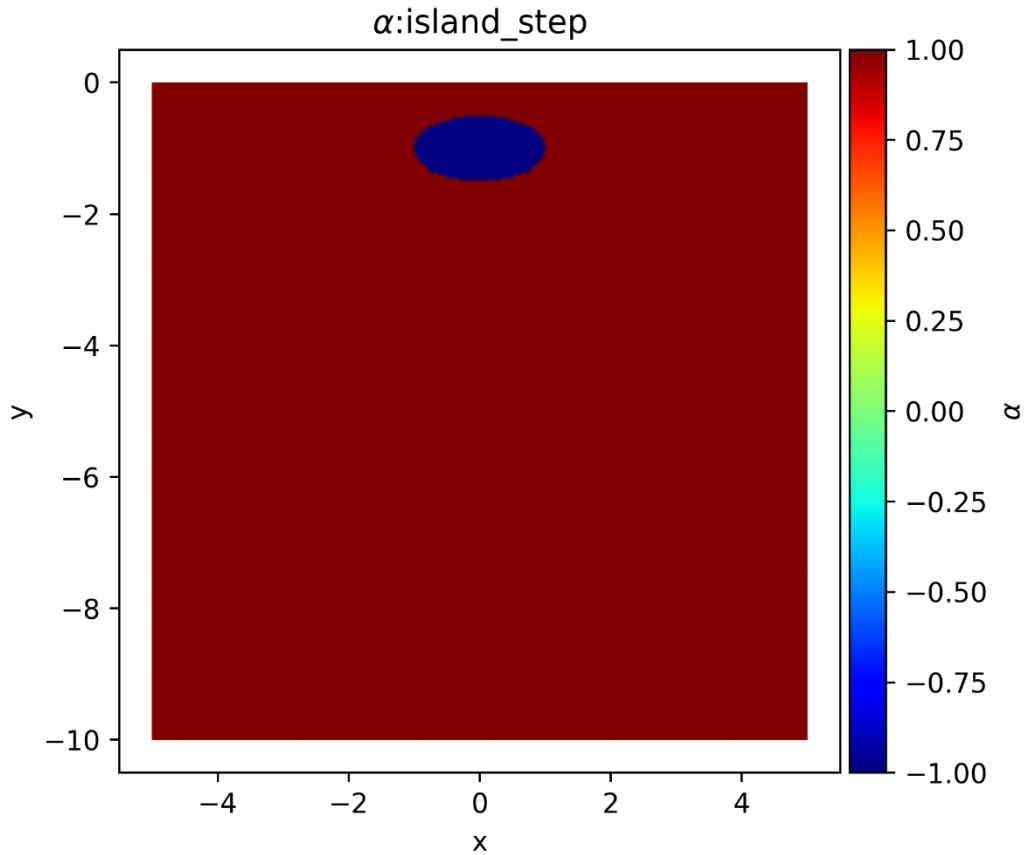


**Figure 2** This representation shows the varying levels of  $\alpha$ - the parameter which determines the superconducting behavior of the material. At  $\alpha=1$ , the material is purely superconducting, while an  $\alpha$  of -1 distinguishes behavior of a regular metal.

## 2.4 Saddle Node Bifurcation to Locate Hsh:

With the program in hand, we can solve for the Ginzburg-Landau equations computationally. The solver identifies when a material leaves its superconducting state, but the purpose of this research is to identify the value of the superheating field (Hsh). Hsh depends on the material, as characterized by  $\alpha$ . We use saddle node bifurcation theory to determine the Hsh of a material. See Alden Pack's master's thesis [5] for more details. In steady state, the

simulation has reached a minimization of the free energy. We then perturb it with a bit of magnetic field and analyze the decay of the perturbation back to a steady state. We infer the time-of-decay to equilibrium,  $\tau$ . The applied field where  $\tau$  equals zero is the super heating field of the material. An extrapolation of the relation of  $\tau$  and the applied field estimates Hsh. A representation of this can be seen in figure 3.

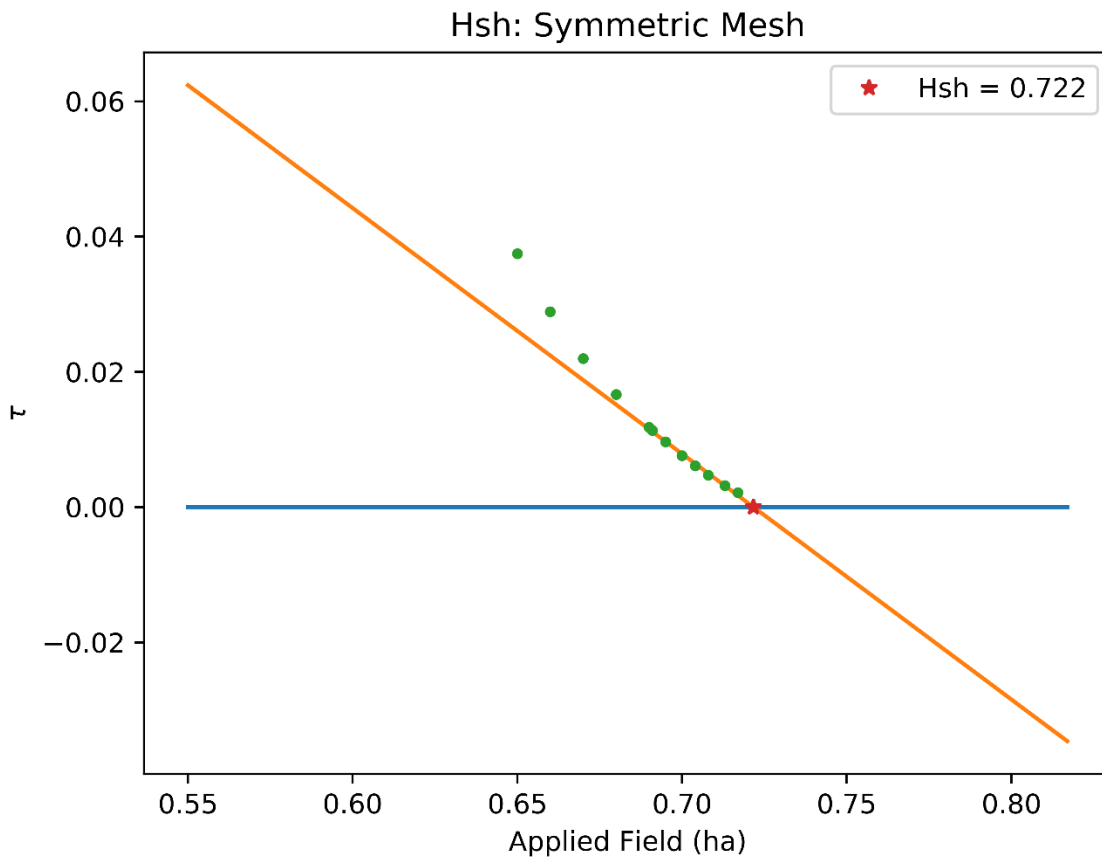


**Figure 3** This graph shows a generic case of different simulations ran at different applied magnetic fields. The value of Hsh is found when the extrapolation of the orange line crosses the blue line held at zero. The extrapolation only uses points that appear linear, which appear closer to zero [4].

For this series of tests, the applied fields that reached a steady state ran from about .65 to .72. For simulations greater than .722, the material quenched and reached a mixed state. The saddle node bifurcation method was not used for cases that reached the mixed state. For the cases where it did not quench, the method determines the decay rate as the applied field increased. As can be seen,  $\tau$  decreased until it almost reaches zero. Near  $H_{sh}$ , the decay is linear, so by extrapolating the linear points we find the value of  $H_{sh}$ , represented by the red star in the graph.

## 2.5 Overview

With this computational development, we can solve the Ginzburg-Landau equations. We used a supercomputer because the methods for solving the equations are computationally expensive. By varying  $\alpha$ , we can distinguish the inhomogeneities of  $Nb_3Sn$ . Upon reaching a steady state, the system is perturbed, and the decay is analyzed to determine at what value of the applied field that the decay rate is zero. At this value of the applied field, we can infer this to be the value of  $H_{sh}$ .

# 3 Results and Conclusions

---

With the computational setup, several simulations were made. All the tests consisted of a tin deficiency island in the center of a field of  $Nb_3Sn$ . The tests incrementally varied the magnetic field from around zero to past where the expected super heating field would occur. The expected super heating fields were calculated by hand, based on the Ginzburg-Landau equations and the material parameters. At each level of magnetic field, the island distance from the boundary also varied. At each distance and magnetic field level where the material did not quench, a perturbation was enforced to distinguish how quickly it would reach a steady state once again.

This secondary test determines where the theoretical super heating field should be, as influenced by the distance of the island from the boundary. Other unique situations were tested afterwards.

### 3.1 Results

#### 3.1.1 Island Size Variations:

Tin island inhomegenties can come in varying sizes, and shapes, and densities. Initial tests consisted of modifying the size of the island in comparison with the rest of the mesh. Obviously, a larger island size corresponds to a larger real-life defect. For these tests, the comparable island size relies on the values of  $\lambda$ . By knowing the value  $\lambda$ , the life-like values can be obtained. Figure 4 shows the data.

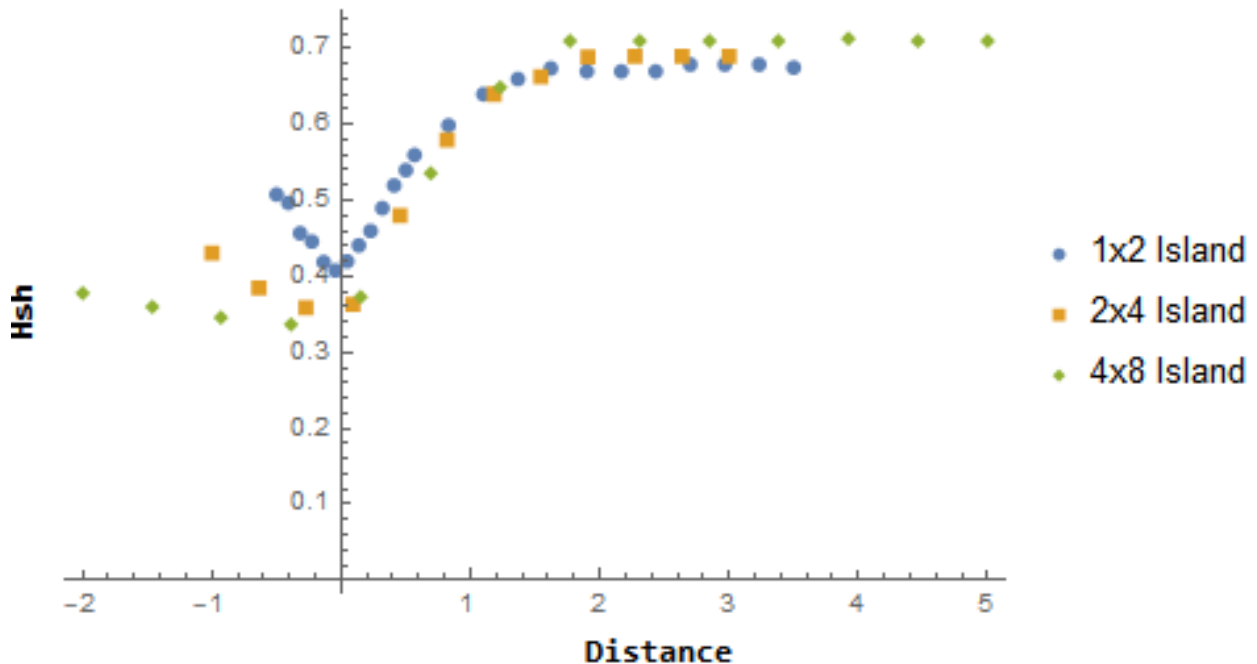


**Figure 4** A plot of the distance of the island and the Superheating field (Hsh) for different island sizes. On the x-axis, is the distance of the island to the boundary in terms of  $\lambda$ , and the y-axis shows the expected super heating field. Notice that for far distances, all the points converge to a value around .72.

The plot has distance on the x-axis and the super heating field (Hsh) on the y-axis. The distance is determined by how far the top edge of the defect is from the top of the grain boundary measured in units of  $\lambda$  for the specific material. In some cases, part of the defect would be exposed and cut off since the deficient island area is outside the superconductor. The negative distances in the graph appear since the ‘top’ of the defect is above the boundary. The smallest value of the distance is where half of the island ellipse is cut off. In this case, only a shape of half of an ellipse has a differing  $\alpha$  value from the rest of the mesh. That is why distance starts off with negative values. The first island tested would be a half island and would be at a distance of -2. (again in terms of  $\lambda$ ), since 2 is half of the ellipse’s vertical diameter. The 2x4 island has data beginning at a distance of -1, and the 1x2 has data at an initial distance of -1/2. For these simulations, the  $\lambda$  of Niobium (50 nm) was used as the basis for units of measurement.

Hsh is where the superconducting phase shift is found to occur. By previous calculations, with a  $\kappa$  of 4, pure superconducting materials are expected to reach a mixed state at a Hsh value of about .72. As seen, this is the value that all the tests converged to when far away from the boundary, regardless of the size of the island. At greater distances, the size of the island proves irrelevant since the material behaves as if no defects were present. At closer lengths, the value of Hsh linearly declines, most likely because of the greater amount of island defects in the material, but when the defect is no longer exposed (at distances that are greater than the island’s vertical radius), it becomes more and more difficult for the magnetic field to enter the material. At longer distances, the material continues to behave as a superconductor under higher magnetic fields until the Meissner state is compromised. The distance where, in all three island sizes, Hsh begins to converge occurs a little below a distance length of two. This point determines where the

closest island defects can be without loss of performance in the superconductor. When fabricated in real life, island defects have yet to be found in ranges lower than the found minimum distance.

### 3.1.2 Alpha Size Variations:

After performing tests varying the size of the island, simulations were made with changes in the parameter  $\alpha$ . Refer back to equation 3 of section 2.1 to remember how  $\alpha$  specifies the superconducting property of the material. When there are greater Tin deficiencies in Nb<sub>3</sub>Sn,  $\alpha$  drops further. Simulations were ran with  $\alpha$  having values of .75, .5, .25, and 0. Similar ranges of distance were used as before, with a consistant island size, 1x2, utilized for all the simulations.

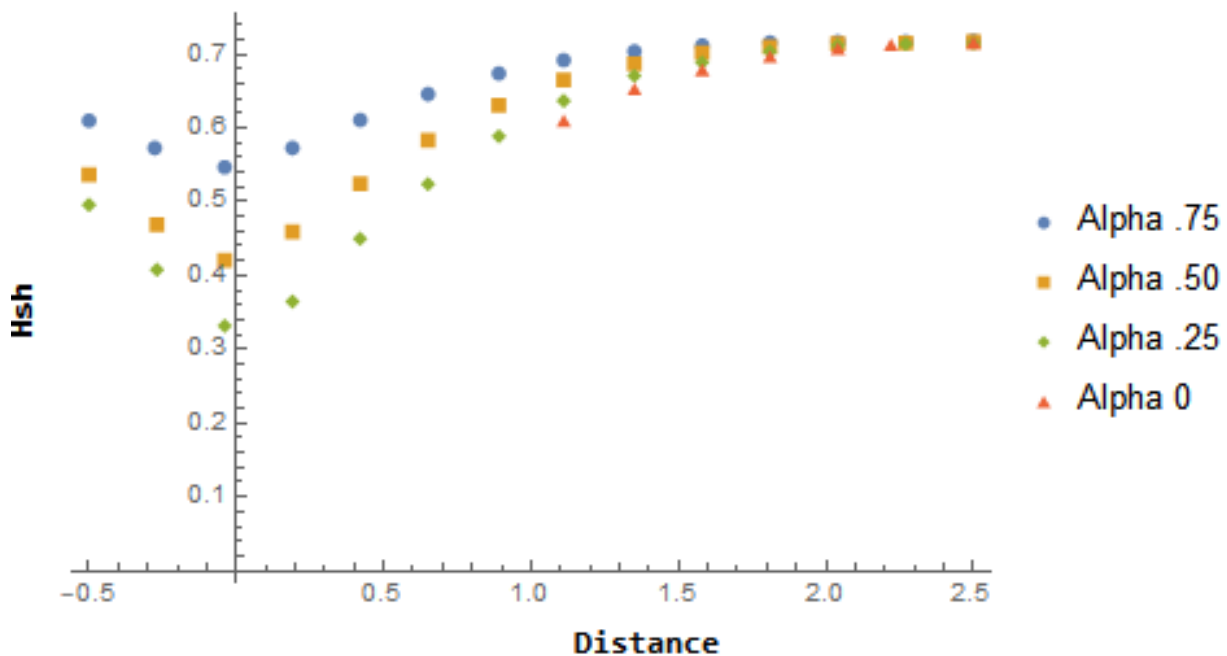


**Figure 5** Plots of Distances versus Super Heating Field with  $\alpha$  differing from 0 to .75.

The same type of behavior as the previous result from the island size variations occurs again. At each  $\alpha$  level, Hsh diminishes linearly until there is some material between the defect and the spatial boundary. At this point, Hsh values begin to curve higher until Hsh once again

converges to values close to .72. Independent of the parameter  $\alpha$ , all data sets clearly converge to the same value. As should be noted, lower  $\alpha$  values of the island cause poorer superconducting performance at closer distances, where the defect can more easily influence performance.

Distances further away are unaffected by islands and their  $\alpha$  levels. At an  $\alpha$  of 0 the simulations broke, and results could not be obtained at lower distance levels. When the code ran smoothly again at larger distances, the partial data set fit perfectly into the established converging pattern, even initially being at lower superheating field values than all the other  $\alpha$  values.

### 3.1.3 Boundary Condition Variations:

With the previous results in hand, further tests were employed to confirm expectations. In this situation, a parameter called the boundary slope was modified. Boundary slope distinguishes how fast a material morphs into the other. Computationally, this is how quickly  $\alpha$  changes from one value to another. Looking at Figure 6, the boundary slope of 1 shifts more gradually from

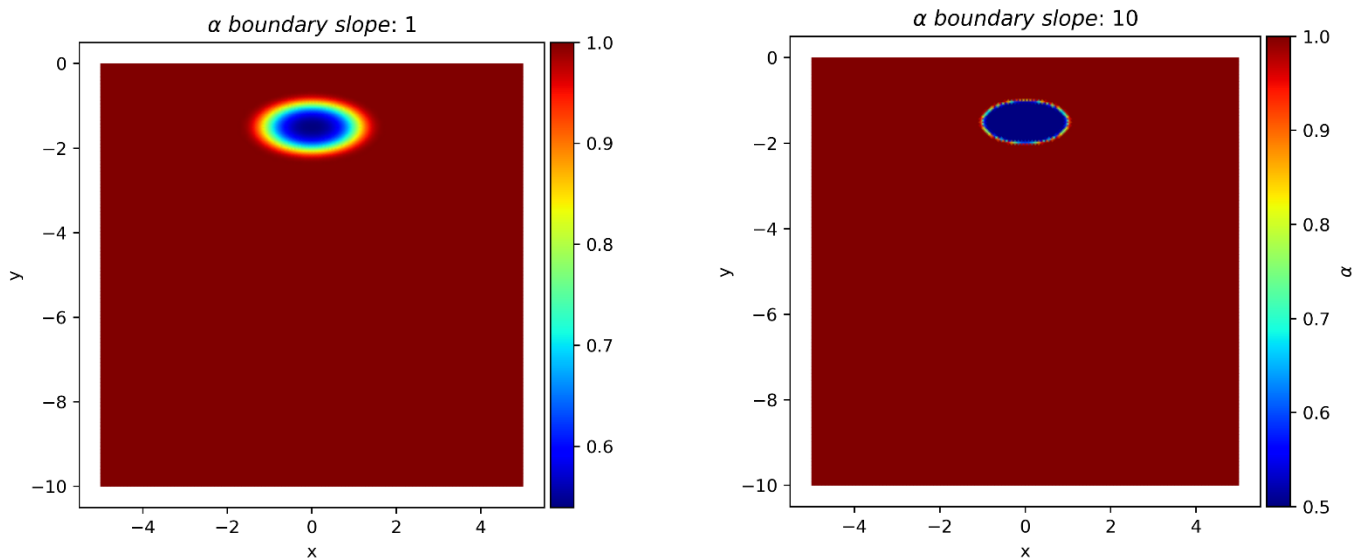


**Figure 6** Plots of two different islands, with a more gradual variation of  $\alpha$  in the left image and a more sharp shift in the image on the right.

one value to another. The boundary slope of 10 more quickly morphs from one  $\alpha$  value to the other. Figure 2 also displays a similar island geometry, but this example has a boundary slope of 10. Testing boundary slopes is important because the script for solving the Ginzburg-Landau equations runs into errors or breaks, unless a gradual shift of  $\alpha$  is used. This possibly deviates from how the materials evolve in real life. Some experimentalists have stated that a sudden shift is possible, while others have discussed an exponential decay from one material to the next. Neither of these theories has been proven [8]. Either way, we can still determine if a more gradual shift or a steep decline can pose any consequence to SRF cavity performance. Furthermore, boundary slope testing will help determine if more efficient computational methods can be used without detrimental effects to the results.

To introduce a gradual change in  $\alpha$ , an error function was utilized, with the high and low ends of the function being held at the  $\alpha$  levels of the two varying materials. A smaller boundary slope is equal to a gradually sloped error function, while a larger boundary slope has a higher rate of change.



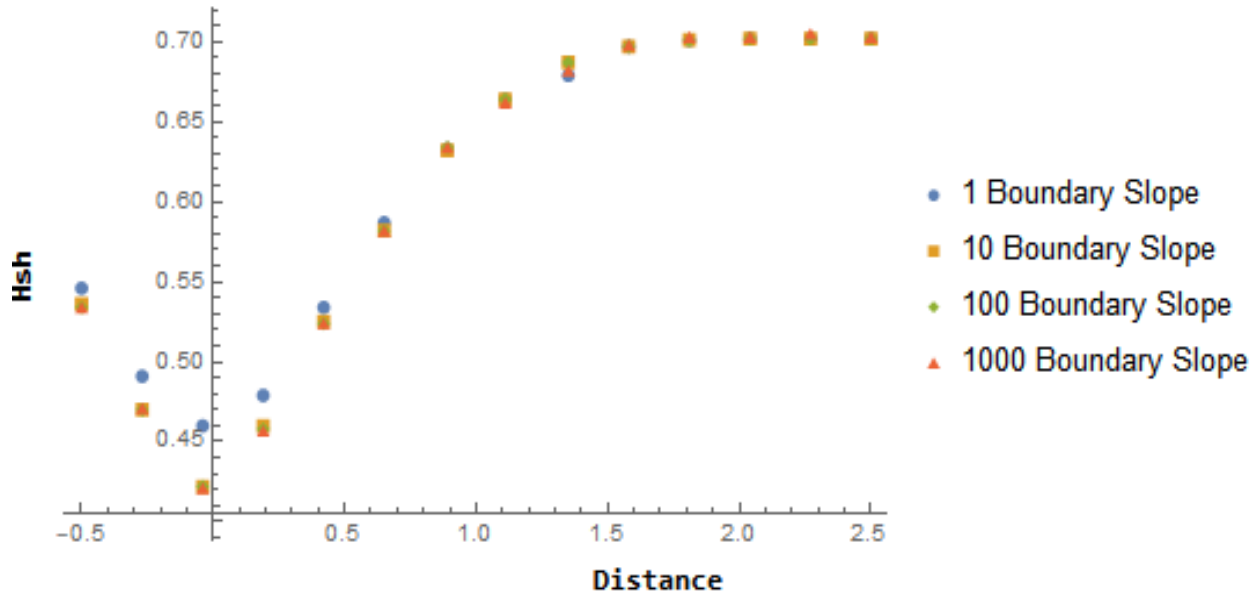


**Figure 7** Distance vs Hsh with altering Boundary Slope values. At larger distances, the points overlap to appear as only one point.

As seen in Figure 7, the boundary slope does not play a significant role in influencing the value of the super heating field. At higher distances, the results overlap and are difficult to distinguish. At smaller distances there is a difference in Hsh between the boundary slope of 1 and the rest of the values. Based on the results, the optimal boundary slope for running the simulations could potentially be 10 or 100 because these values produce the most similar results, while still minimizing computational pitfalls.

## 3.2 Conclusion

The goal of this research sought to determine Nb<sub>3</sub>Sn as a suitable replacement for Niobium. Three separate sets of simulations were ran targeting certain variations in experimental design. By running tests of changing island size we concluded that the Sn-deficiency defects do not pose any threat on performance, as long as the island remains at a sufficient distance. Tests

altering the superconducting properties ( $\alpha$ ) of the defecting material were also performed. These tests verified that percentage of Tin deficiency plays no role in the performance of the superconducting cavity. Furthermore, additional tests were ran to check the validity of the boundary slope approach as a solution to potential computational complications with the setup of the mesh.

The graphs of super heating field all contained the same basic pattern, confirming the reliability of the methods used to identify the superconducting performance. The convergence of Hsh at .72 also served as a great indication of the validity of the used methods. It is encouraging to note that islands at longer distances did not cause any detrimental effects on how well the material expelled magnetic fields. As of now, no islands have been found below distances where Hsh converges. It would be advisable for experimentalists to verify that no islands actually exist at distances below the convergence point.

### **3.3 Future Work**

There are still many tests and variations of these simulations that still must be solved to verify Nb<sub>3</sub>Sn as an alternate material for Nb. The paramters  $\alpha$  and  $\beta$  were used. It would be highly beneficial to simulate these results with more accurate material variables that are based on physical phenomenon, instead of these more simple values. Some parameters to include as input to characterize the material are coherence length, penetration depth, critical temperature, and the critical magnetic field. The Ginzburg-Landau equations can be modified to incorporate these variables into code. Some progress has been made in our research group in constructing more descriptive forms of these equations.

Likewise, other geometries other than ellipses should be analyzed. Especially those that naturally occur by fabrication. One of these geometries could be a layer of Nb<sub>3</sub>Sn on top of a layer of Nb. If proved beneficial towards performance, the layers could provide a more cost-effective method for fabrication. Also, simulations were performed only in two dimensions. To better mimic natural behavior, 3D simulations could prove beneficial for understanding the superconducting material.

Many further studies can be done. Effective mass can be analyzed, as well as variations in the temperature gradient. Analyzing even more complex geometries is a future area of study, as well as looking at different directions of the external magnetic field. All of these cases aid in concluding the utility of Nb<sub>3</sub>Sn as the next superconducting material to form SRF cavities.

# 4 Index

---

Coherence length, 11, 27

FEM, 14

FEniCS, 14

Ginzburg-Landau, i, iii, 11, 12, 14, 15, 17, 20, 25, 27, 30

Introduction to Superconductivity, 15

London Penetration Depth, 10

Meissner effect, 9, 30

Order Parameter, 15

Saddle Node Bifurcation, 18, 19

SRF, vii, 9, 12, 14, 30

Type 1, 10

Type II, 10, 12

Vortices, 9

# 5 Bibliography

---

- [1] Posen, S. (2015). *Understanding and overcoming limitation mechanisms in Nb<sub>3</sub>Sn superconducting RF cavities*.
- [2] Harbick, A. V. (2020). *Computational Simulations of Temperature-dependent Dynamics in Type II Superconductors Using a Material Specific Formulation of Ginzburg Landau Theory* (Doctoral dissertation, College of William and Mary).
- [3] Posen, S., & Hall, D. L. (2017). Nb<sub>3</sub>Sn superconducting radiofrequency cavities: fabrication, results, properties, and prospects. *Superconductor Science and Technology*, 30(3), 033004.
- [4] J. Carlson, Senior Thesis, 2019.
- [5] Alden Pack, Senior Thesis, 2015.
- [6] Alden Pack, Master's Thesis, 2017.
- [7] M. Tinkham, Introduction to superconductivity (McGraw-Hill, New York, 1975), Chap. 1-4.  
S Posen and D L Hall 2017 *Supercond. Sci. Technol.* **30** 033004
- [8] M. "Transtrum, "personal communication".